AJDS LAZHAR Al-Azhar Journal of Dental Science Print ISSN 1110-6751 | online ISSN 2682 - 3314
Vol. 27- No. 4- 535:547- October 2024 https://ajdsm.journals.ekb.eg
Oral Biology, Medicine & Surgical Sciences Issue *(Oral Biology, Oral Pathology, Oral Periodontology, Medicine, Oral & Maxillofacial Surgery)*

THERAPEUTIC EFFICACY OF AXITINIB AS ANTI-ANGIOGENESIS AND NIVOLUMAB AS IMMUNOTHERAPY ON DMBA INDUCED HAMSTER BUCCAL POUCH CARCINOMA UTILIZING VASCULAR ENDOTHELIAL GROWTH FACTOR

Salah Gamal El-Sawy[1*], Emad Soliman Al-qalshy[2], Mohamed Gomaa Attia Zouair[3]

ABSTRACT

Objective: This study aimed to determine the therapeutic efficacy of axitinib as anti-angiogenesis and nivolumab as immunotherapy on 7,12-dimethylbenz (a) anthracene (DMBA) induced hamster buccal pouch (HBP) carcinoma visualized by immunohistochemistry. **Subjects and methods:** Fifty Syrian male hamsters were classified into five equal groups (s) (G(s)) of ten each. GI: The animals act as negative controls. The right pouches of animals in other groups were painted three times a week for 14 week (s) with DMBA. GII: No additional treatment.in GIII were injected intraperitoneally (IP) with nivolumab (200 µL on days 7, 10, and 13), in GIV were given axitinib by oral gavage at a dose as a suspension at 5 mL/kg orally twice daily for 4 weeks, in GV were received a combination of nivolumab and axitinib with doses and administration method similar to those introduced in single treatments. After termination of the experiment, gross observations were recorded, then, the animals were euthanized, all pouches were surgically excised, fixed and processed for hematoxylin and eosin (H&E) stain examination, immunohistochemical (IHC) staining utilizing vascular endothelial growth factor (VEGF) as angiogenic marker. **Results:** the results revealed some variability across the medicated groups contrasted to GII. VEGF IHC revealed highly significant difference between GI & GII, GII& GV, GV & GIII and GV & GIV (p value < 0.001). Moreover, there was highly significant difference between GIII and GIV (p value < 0.001). **Conclusion:** Combinatorial effect of axitinib-nivolumab significantly inhibits tumor progression and induces apoptosis in DMBA induced HBP carcinoma.

KEYWORDS: nivolumab, axitinib, HBP carcinoma.

INTRODUCTION

Oral tumor is considered the sixth most widespread cancer globally. Oral cancer generally grows from hyperplasia to carcinoma as it progresses through the characteristic multistep carcinogenesis of cascading growth of genetic amendments ensuing in irregular cellular appearance, carcinoma, and deregulation of cell growth[(1)].

The valuable knowledge about carcinogenesis has been developed throughout the experimental research on animal model. Accumulated evidences pointed out the successful results when utilizing

1. Assistant Lecturer, Oral and Dental Pathology Department, Faculty of Dental Medicine (Boys- Cairo), Al-Azhar University, Egypt.
2. Lecturer, Oral and Dental Pathology Department, Faculty of Dental Medicine (Boys- Cairo), Al-Azhar University, Egypt.
3. Professor, Oral and Dental Pathology Department, Faculty of Dental Medicine (Boys-Cairo), Al-Azhar University, Egypt.

• ***Corresponding author*:** elsawy623@gmail.com

DOI: *10.21608/ajdsm.2023.190759.1417*

histological, biochemical, immunohistochemical and molecular investigations on 7,12-dimethylbenz (a) anthracene (DMBA) induced hamster buccal pouch (HBP) carcinoma[2].

The immune responses, especially the cell-mediated immunity, play an important role to recognize and delete tumor cells. However, cancer cells can escape from the immune system by some regulatory mechanisms such as upregulating immune inhibitors of immune checkpoints in T lymphocytes. Immune checkpoints are normal immune signals which can stop an immune response [3]. The most effective immune checkpoint blocker developed in recent years is antibodies against programmed cell death (PD)-1 and its ligands (PD-L1) called nivolumab[4].

Nivolumab, an immune checkpoint inhibitor that acts by preventing PD-L1 from binding to PD-1 receptor, is utilized to treat a variety of cancers including renal cell carcinoma, non-small cell lung cancer, and metastatic melanoma. Currently, nivolumab is US Food and Drug Administration (FDA) approved as a second- line treatment for advanced hepatocellular carcinoma[5].

The progression of oral dysplastic lesions into OSCC is characterized by an increase in neovascularization (angiogenesis), which can be considered as an indicator of malignant transformation[6]. Angiogenesis is a process by which development of new blood vessels from existing vasculature, physiologically it occurs in normal embryonic development, wound healing and also certain angiogenesis occurs pathological such as chronic inflammation, immune reaction, premalignancy and malignancy[7].

The most important factors associated with angiogenesis include vascular endothelial growth factor (VEGF), platelet derived growth factor, and fibroblast-derived growth factor. Vascular endothelial cells depend for their survival on serum VEGF, which stimulates proliferation and migration, inhibits apoptosis, and modulates endothelial permeability. Antiangiogenic therapy aims to disrupt those processes by normalizing the abnormal vasculature in cancer, improving delivery of chemotherapy, enhancing its antivascular effect, and preventing rapid repopulation after systemic treatment[8]. Axitinib is an orally available high affinity tyrosine kinase inhibitor of the VEGF receptors, blocking VEGF-R-1, -2 and -3. It is approved by the FDA and the European Medicines Agency (EMA) for the treatment of patients with recurrent metastatic renal cell carcinoma[9]. Axitinib has an anti-angiogenic and survival prolongation effect in preclinical glioblastoma models and inhibits tumor growth in a glioblastoma xenograft model[10].

Thus, the primary aim of this study was to determine the effects of nivolumab and/or axitinib on DMBA induced HBP carcinoma. The evaluation depends on the animal's general health examinations, HBP gross observations, histological tumor tissue changes and immunohistochemistry (IHC) examinations.

SUBJECTS AND METHODS

Chemicals

DMBA (0.5%) was gathered from Sigma-Aldrich company, solubilized in paraffin oil. Nivolumab (trade name Opdivo; Bristol-Myers Squibb company, USA), was prepared by redispersing vial solution in 0.9% sodium chloride (10 mg/ml). Axitinib (Sigma-Aldrich company, USA), was prepared by redispersing vial solution in 0.5% carboxymethylcellulose/H2O_HCl[11].

Animals

Fifty Syrian male hamsters, weighing between 80 and 120g, and five weeks old. The experimental hamsters were kept in standard boxes with sawdust bedding in a controlled environment with humidity (30-40%), temperature (20 ±2°C), and light (12-hour light/12-hour dark). A healthy hamster walks regularly and smoothly, had bright, clear eyes, healthy skin, and a soft, lustrous coat devoid of parasites, wounds, dry spots, and swellings.

Ethical Approval

Ethical approval cleared by ethical committee of Faculty of Dental Medicine (Boys- Cairo), Al-Azhar University, Egypt (Ethical Code No. 172/254/07/09/19)

Experimental design

The animals were randomly categorized into five groups (Gs), 10 each. After a week of adaptation. The right pouches of the animals in GII, GIII,GIV and GV were painted three times a week for 14 weeks with 0.5% DMBA in liquid paraffin by a number 4 camel's hairbrush[2], whereas the animals in GI (negative control) were kept untreated. Following that, the animals in GII (positive control) not received other treatment while those in GIII (nivolumab) were injected intraperitoneally (IP) by insulin syringe with nivolumab (200 µL on days 7, 10, and 13), on day 22, the animals were euthanized [2]. The animals in GIV (Axitinib) were given by oral gavage at a dose as a suspension at 5 mL/kg orally twice daily for 4 weeks with axitinib. Then, after 2 weeks, the animals were euthanized [11], while those in GV (Axitinib - nivolumab) the animals were received a combination of nivolumab and axitinib with doses and administration method similar to those introduced in single treatments.

General health examinations

The alterations in the animal's general health were monitored throughout the experiment. Hamsters that demonstrated any of the following signs (crowding in sneezing, anorexia, silence, corner, diarrhea, discharge from the nose or eyes, dampness around the tail, wheezing, and hair loss) of illness or disease were adapted.

Tumor volume measurement:

After termination of the experiment, gross observations of HBP mucosa were recorded (mucosal thickness, exudation, ulcers, and tumors). Then, the animals were euthanized, the right cheek pouch everted, and the diameter of each tumor was measured with a Vernier caliper. The tumor volume, where the three diameters (mm) of the tumor are D1, D2 and D3, was calculated by the formula, $Vmm3 = (4/3)\ \pi\ [(D1/2)\ (D2/2)\ (D3/2)]$[2].

Sample collection and preparation

The right cheek pouch was excised, fixed in 10% neutral buffered formalin, routinely processed, and embedded in paraffin blocks to be examined histologically and IHC utilizing VEGF.

Histopathological examinations

Utilizing a rotary microtome, 4 **µm** thick tissue sections were cut from paraffin blocks, processed, mounted on glass slides, and stained with Hematoxylin and Eosin (H&E) for light microscopic inspection.

Measurement of the depth of invasion (DOI)

The DOI of all surgical specimens was determined using the H&E slide. The DOI was calculated from the surface epithelium's basal layer to the deepest point of tumor infiltration. According to the American joint committee of cancer (AJCC), it is further characterized as less invasive at ≤5 mm, moderately invasive at 6-10 mm, and highly invasive at ≥10 mm [12] (Fig.1). The DOI was determined by a Leica QWIN V3 image analyzer computer system (Switzerland), which was operated via the Leica QWIN V3 software. This was done in Oral and Dental Pathology Department, Faculty of Dental Medicine (Boys-Cairo), Al-Azhar University, Egypt.

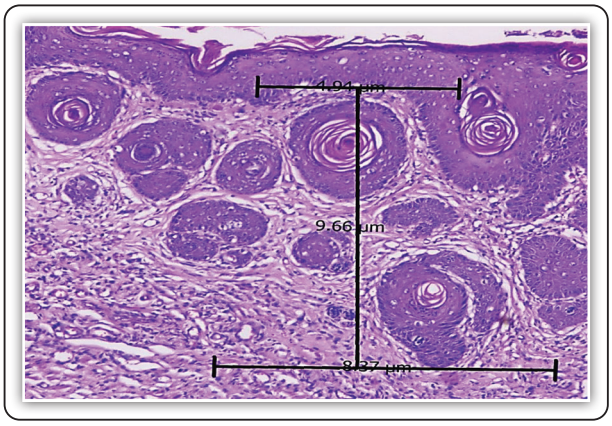

FIG (1) Photograph of measuring the DOI, the greatest invasion was measured by dropping a "plumb line" from the horizon to the deepest invasive nest.

Immunohistochemical examination [13]

Other tissue sections were cut at 4μm and put on positive charged slides for the application of standard labeled streptavidin- biotin method to demonstrate the expression of VEGF antibody. The sections were deparaffinized in xylene and rehydrated through graded ethanol (100%, 95 % and 70 %) each run for 5 minutes. Slides were washed in distilled water then in phosphate buffered saline (PBS), each for 5 minutes. Endogenous peroxidase activity was blocked using 3% solution of hydrogen peroxide (H2O2) in methanol for 30 minutes at room temperature. Slides were then washed in PBS. Slides were then immersed in plastic jars containing 200 ml of citrate buffer (pH 6). The jars were put in microwave at maximum power at 100°C for 3 intervals, each one 5 minutes. Slides were left at room temperature to coal gradually. Slides were then washed in distilled water followed by PBS for 5 minutes. Tissue sections were received one or two drops of the primary antibody (VEGF) in a dilution of 1:100 and incubated in a humid chamber at room temperature overnight. Slides were then washed in distilled water, followed by PBS for 5 minutes. Biotinylated secondary antibody was added and incubated at room temperature for 30 minutes. Tissue sections were then washed in PBS for 5 minutes. One or two drops of peroxidase-labeled streptavidin were applied for 30 minutes at room temperature then washed in PBS. The tissue sections were received DAB for 2-4 minutes to develop color, followed by putting in distilled water. Tissue sections were counterstained using Mayer's hematoxylin for one minute and then washed in tap water. The slides were placed in two changes of 95% alcohol followed by two changes of absolute alcohol, each for 3 minutes then mounted with DPX and covered with plastic covers in order to be examined. Negative controls were prepared by omitting the primary antibody. Liver tissues were used as positive controls for VEGF and the immunostained sections were examined using light microscope to assess the prevalence of positive cases and the localization of immunostaining within the tissues. In addition, image analysis computer system was used to assess area percentage of VEGF positive cells of the immunostaining. This was done in Oral and Dental Pathology Department, Faculty of Dental Medicine (Boys-Cairo), Al-Azhar University, Egypt.

Statistical analysis

The data were statistically examined, and the mean and standard deviation were calculated (SD). A one-way analysis of variance was performed using SPSS version 17.0 for Windows (ANOVA). With quantitative data and parametric distribution, ANOVA was utilized to differentiate between more than two separate groups, accompanied by post hoc analysis with the LSD test. To establish significance, the relevant p-values were used: p 0.05: significant, $p > 0.05$: non-significant, and $p< 0.001$: extremely significant.

RESULTS

Gross observations

GI examination revealed no obvious alterations, neither hair loss or skin ulcerations. The HBP was normal pale pink with no pathological or inflammatory signs, their buccal pouch length was from (5-5.5) cm (Fig. 2A). In **GII**, all hamsters demonstrated debilitation and observable hair loss with para-oral skin ulcerations. Large exophytic growths with prominent vascularity in the animals' pouches, in addition to eroded, and ulcerative areas with spontaneous bleeding were seen (Fig. 2B). The mean tumors volume measurement of tumor-bearing animals in ten animals in **GII** was 779.5 mm3 (620 – 1005 mm3), and the pouch length in **GII** recorded from (1.5-2 cm). In **GIII and GIV,** all hamsters showed slight improvement in the general health compared to the animals in GII. The length of the pouches was 2.5-3.5cm with reduction of distal necrosis. The right HBP mucosa showed various changes, multiple exophytic masses of small sizes surrounded with areas of ulceration and bleeding (GIII: 5 hamsters while GIV: 6 hamsters), small exophytic nodule with absence

of ulceration and bleeding (GIII: 3 hamsters while GIV: 4 hamsters) and whitish membrane leaving thick erythematous and hemorrhagic area (GIII: 3 hamsters), **(Fig.2C&D)**. There was a decrease in the mean tumor volume of GIII (459.5mm3) and (409.5 mm3) compared to that of GII. In **GV,** all hamsters showed marked improvement in general health compared to the animals in GII. Only 2 hamsters out of 10 had perioral skin ulcers and hair loss. The other 8 hamsters, hair started to grow again in the unhaired areas. All hamsters regain their appetite and activity. There was a significant increase of the pouch's length ranged from 3.5-4.5cm with no distal necrosis. The right HBP mucosa showed various changes, 3 hamsters out of 10 showed small exophytic nodule with absence of ulceration and bleeding, 5 hamsters showed whitish membrane leaving thick erythematous and hemorrhagic area, while 2 hamsters showed demarked grayish white patch. There was a marked decrease in the size of exophytic growths in this group when compared to those either in the treated Gs (GIII & GIV) or GII. There was marked decrease in the mean tumor volume of GV (28.6 mm3) compared to either in the treated Gs (GIII & GIV) or GII **(Fig.2E)**.

Regarding **tumor volume**, there was highly significant difference (p value < 0.001) between GII and the treated Gs (GIII, GIV& GV). Comparing the various treated groups, GV showed highly significant difference (p value < 0.001) with either GIII or GIV. Furthermore, there was significant difference (p value =0.014 between GIII and GIV,) **(Table. 1 & Fig. 3).**

FIG (2) A- Photograph of GI showing normal buccal pouch mucosa which appeared pink in color with smooth surface (arrow). **B-** Photograph of GII showing multiple exophytic papillary tumor masses surrounded with bleeding areas (arrow). **C-** Photograph of GIII showing small tiny elevation with absence of ulceration and bleeding (arrow). **D-** Photograph of GIV showing small size nodule with absence of ulceration and bleeding (arrow). **E-** Photograph of GV showing marked decrease in the size of tumor masses with absence of ulceration and bleeding (arrow).

TABLE (1) Comparison between the studied groups as regard to tumor volume.

	Tumor volume	**P-value for post analysis using LSD test**			
	Mean ± SD	**GII**	**GIII**	**GIV**	**GV**
GII	779.5 ± 25.03	--	0.000	0.000	0.000
GIII	459.5 ± 13.46	0.000	--	0.014	0.000
GIV	409.5 ± 22.10	0.000	0.014	--	0.000
GV	28.6 ± 3.18	0.000	0.000	0.000	--
F			**2794.805**		
P-value			**<0.001 (HS)**		

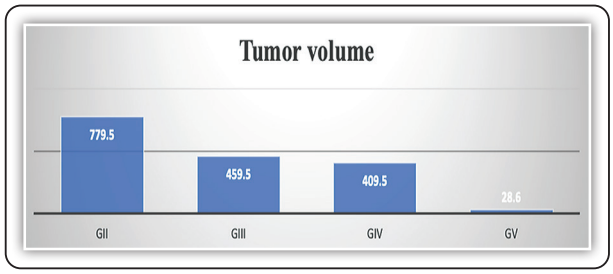

FIG (3) Comparison between the studied groups regarding tumor volume level.

Histological and IHC findings:

The **GI** exhibited a normal thin stratified squamous epithelium with minor keratinization, consisting of 2-3 layers of squamous cells. A subepithelial connective tissue and a muscle layer were discovered **(Fig.4A)**. The IHC staining using VEGF antibody exhibited positive cytoplasmic expression (mean = 19.70 %) which present in almost all normal epithelial cells, which was predominantly detected in the basal layer **(Fig.4B).**

GII: The overlying epithelium revealed multiple areas with dysplastic feature including basilar hyperplasia, hyperchromatism, loss of polarity, large nucleoli, altered N/C ratio, and cellular and nuclear pleomorphism, Destructive basement membrane with invasive epithelial islands into the underlying connective tissue. **(Fig.4C).** The mean DOI revealed 10.7mm. The IHC staining using VEGF antibody exhibited positive cytoplasmic expression (mean= 70.20 %) throughout the epithelial layers and invading tumor cells **(Fig. 4D).**

GIII: In 5 hamsters out of 10, exhibited different degrees of epithelial dysplasia, one hamster revealed moderate epithelial dysplasia, 2 hamsters displayed severe epithelial dysplasia and 2 hamsters displayed carcinoma in situ (CIS). In contrast, the other 5 hamsters had well-differentiated SCC that had not progressed to the deeper parts. Distal necrosis was reduced, inflammatory infiltration was decreased, and the amount of keratin formation and collagen fibers were increased **(Fig.4E)**. The mean DOI in GIII (10 hamsters) was 1.7mm. The IHC staining using VEGF antibody exhibited positive cytoplasmic expression (mean=51.80 %) throughout the epithelial layers and invading tumor cells **(Fig. 4F).**

GIV: In 5 hamsters out of 10, exhibited different degrees of epithelial dysplasia, 2 hamsters displayed severe epithelial dysplasia and 3 hamsters displayed CIS. In contrast, the other 5 hamsters had well-differentiated SCC that had not progressed to the deeper parts. Distal necrosis was reduced, inflammatory infiltration was decreased, and the amount of keratin formation and collagen fibers were increased **(Fig.4G)**. The mean DOI in GIV (10 hamsters) was 1.8mm. The IHC staining using VEGF antibody exhibited positive cytoplasmic expression (mean= 42.40%) throughout the epithelial layers and invading tumor cells **(Fig. 4H).**

GV: In 7 hamsters out of 10, exhibited different degrees of epithelial dysplasia, one hamster revealed mild epithelial dysplasia, 3 hamsters revealed moderate epithelial dysplasia, 2 hamsters displayed severe epithelial dysplasia and one hamster displayed CIS. In comparison, the remaining 3 hamsters exhibited well-differentiated SCC that did not extend to the deeper connective tissue, the connective tissue exhibited a reduction in distal necrosis, a marked decrease in inflammatory infiltration, and an elevation in the thickness of the striated muscle layer. At the same time, a few tumor masses were substituted by proliferating fibrous tissue with enhanced collagen deposition **(Fig.4I)**. The mean DOI in GV was 0.8mm. The IHC staining using VEGF antibody exhibited positive cytoplasmic expression (mean= 26.8%) throughout the epithelial layers and invading tumor cells **(Fig. 4J).**

Regarding DOI, there was highly significant difference (p value < 0.001) between GII and the treated Gs (GIII, GIV& GV). Comparing the various treated groups (GIII, GIV, and GV), GV showed non-significant difference with either GIII or GIV, (p value = 0.073, 0.204 respectively). Furthermore, there was non-significant difference (p value = 0.583) between GIII and GIV, (Table. 2 & Fig. 5).

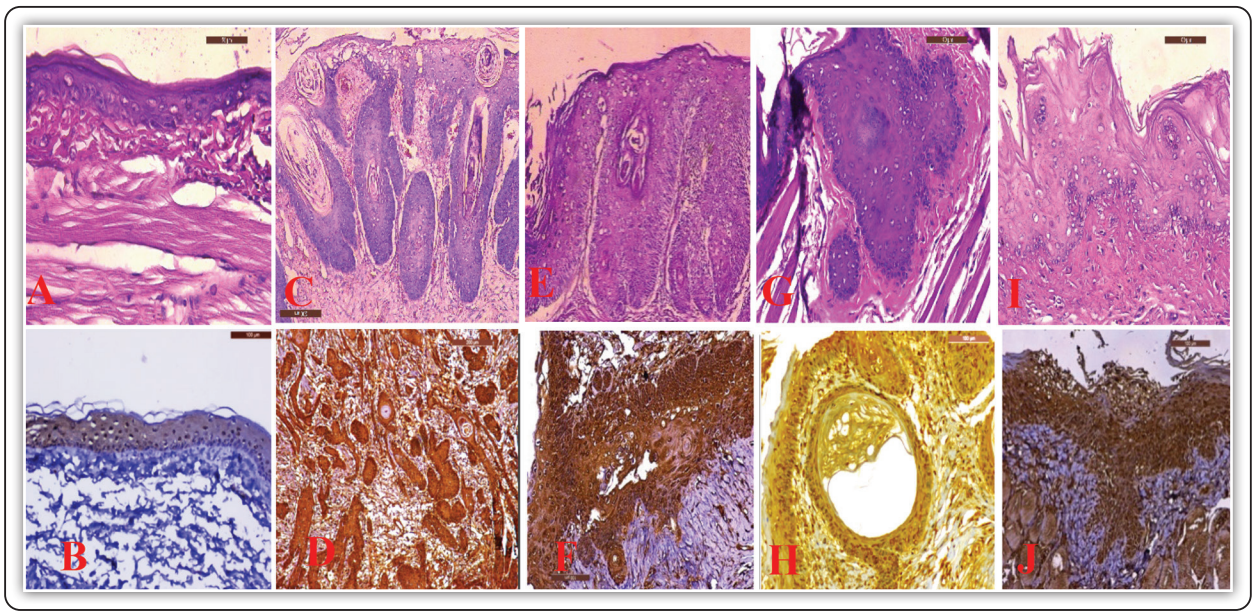

FIG (4) **A-** Photomicrograph of GI showing epithelium consists of two to four layers, superficial squamous cells exhibiting keratinization, flattened rete ridges, C.T layer, muscular layer, and deep layer of loose areolar connective tissue (H&E stain X400). **B-** The IHC staining using VEGF antibody exhibited positive cytoplasmic expression in almost all normal epithelial cells. **C-** Photomicrograph of GII showing well differentiated SCC with deep invasion of multiple tumor islands into the underlying connective tissue and sub-epithelial inflammatory infiltrates (H&E stain X100).**D**- The IHC staining using VEGF antibody exhibited positive cytoplasmic expression throughout the epithelial layers and invading tumor cells**. E-** Photomicrograph of GIII showing well differentiated SCC (superficial invasion)(H&E stain X400). **F-**The IHC staining using VEGF antibody exhibited positive cytoplasmic expression throughout the epithelial layers and invading tumor cells(arrow).**G-**Photomicrograph of GIV showing well differentiated SCC (superficial invasion)(H&E stain X200).**H-** The IHC staining using VEGF antibody exhibited positive cytoplasmic expression throughout the epithelial layers and invading tumor cells. **I-** Photomicrograph of GV showing severe dysplasia with hyperkeratosis (H&E stain X200).**J-**The IHC staining using VEGF antibody exhibited positive cytoplasmic expression throughout the epithelial layers and invading tumor cells.

TABLE (2) Comparison between studied groups with regard to DOI.

	DOI	**P-value for post analysis using LSD test**			
	Mean ± SD	**GII**	**GIII**	**GIV**	**GV**
GII	10.70 ± 1.93	--	0.000	0.000	0.000
GIII	1.70 ± 1.07	0.000	--	0.583	0.073
GIV	1.80 ± 0.88	0.000	0.583	--	0.204
GV	0.80 ± 0.46	0.000	0.073	0.204	--
F			134.250		
P-value			<0.001 (HS)		

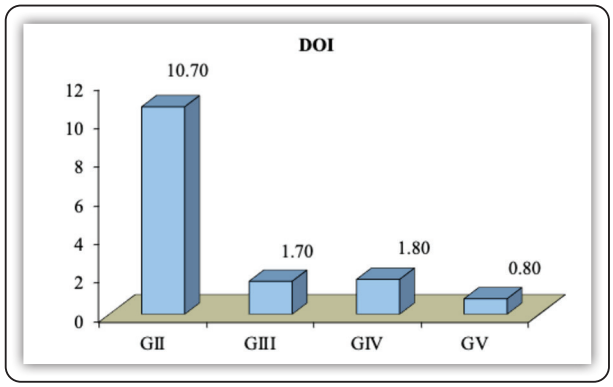

FIG (5) Comparison between the studied groups regarding DOI level.

Regarding VEGF, there was highly significant difference between GI& GII (p value < 0.001). Comparing the positive control group (GII) with the various treated groups (GIII, GIV, and GV), there was highly significant difference between GII& GV (p value < 0.001). Comparing the various treated groups (GIII, GIV, and GV), GV showed highly significant difference (p value < 0.001) with either GIII or GIV. Furthermore, there was highly significant difference (p value < 0.001) between GIII and GIV (Table. 3 & Fig. 6).

TABLE (3) Comparison between the studied groups regarding VEGF level

	VEGF	**P-value for post analysis using LSD test**				
	Mean ± SD	**G1**	**GII**	**GIII**	**GIV**	**GV**
GI	19.70 ± 3.40	--	0.000	0.000	0.000	0.000
GII	70.20 ± 3.72	0.000	--	0.000	0.000	0.000
GIII	51.80 ± 4.00	0.000	0.000	--	0.000	0.000
GIV	42.40 ± 4.19	0.000	0.000	0.000	--	0.000
GV	26.80 ± 2.89	0.000	0.000	0.000	0.000	--
F	**300.392**					
P-value	**<0.001 (HS)**					

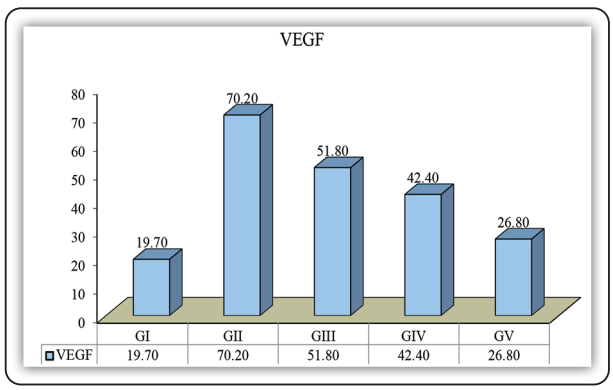

FIG (6) Comparison between the studied groups regarding VEGF level.

Correlation analysis:

There was a statistically significant positive (direct) correlation between tumor volume and area % of VEGF expressions (p value < 0.001) (**Table. 4, Fig. 7**). This means that an increase in one variable is associated with an increase in the other variable and vice versa.

TABLE (4) Correlation of area % of VEGF with tumor volume in all the studied groups.

	Correlation coefficient (r)	**p-value**
Tumor volume vs area % of VEGF	0.907	0.000

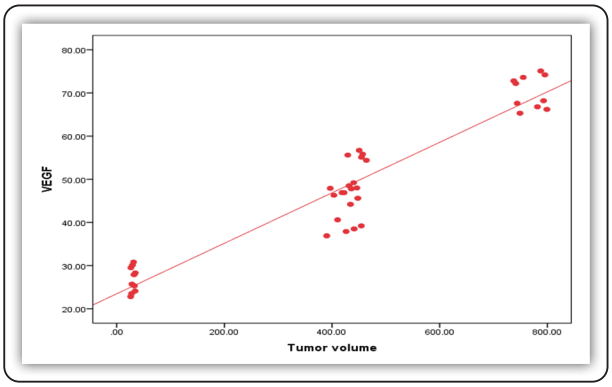

FIG (7) Correlation of tumor volume with area % of VEGF expressions.

DISCUSSION

To address whether value of axitinib as antiangiogenesis and/or nivolumab as immunotherapeutic drugs for treatment and inhibition of tumor progression of DMBA induced hamster buccal pouch carcinoma, this study was done. To our knowledge, in the open English literatures, this was the first study to evaluate the effect of nivolumab and/or axitinib on DMBA induced HBP carcinoma. The results of animal's general health examinations, HBP gross observations, H&E stain and IHC examination, revealed variable observations.

In the current study, GII showed marked perioral hair loss, pouch depth decrease, skin ulcers and marked debilitation of all animals. Animal's pouches showed large exophytic growths with pronounced vascularity and the pouch length (1.5-2cm) which was decreased compared to GI due to necrosis in the distal end of the pouch. These observations are mainly due to the strong toxic DMBA effect[14]. By using H&E stain, a development of various patterns of invasive SCC (50% well differentiated and 50% moderately differentiated) were seen which extended to deeper areas of C.T (DOI=10.7mm). This is in consistence with that shown by other researchers[15, 16]. These findings may be referred to higher level of intracellular ROS during DMBA application which may be attributed to repeated exposures to tumor promoters create a chronic inflammatory state with a sustained release of ROS, which results in chronic oxidative stress. Free radicals and non-radical ROS such as H_2O_2 released by phagocytic cells can cause damage, such as DNA strand breaks, mutations, sister chromatid exchanges, protein modifications and lipid peroxidation, to adjacent epithelial cells. In addition, protein modifications induced by free radicals/ROS can affect DNA repair capacity, transcriptional regulation, apoptosis, metabolism and cell signaling[17].

In the current study, IHC staining of GII showed positive cytoplasmic expression of VEGF (70.20 %) that was seen throughout the epithelial layers and invading tumor cells, that showed highly significantly expression compared to GI (p value < 0.001). This result is in agreement with that of other investigator[18, 19]. Martano et al[20] identified a significant increase in VEGF expression during the transition between normal and OSCC tissues, in association with an increasing grade of differentiation. This was indicated by a high number of VEGF-positive cells associated with the accumulation and consequent loss of cytoplasmic polarization of VEGF granules in less differentiated tumors. Johnston et al[21], indicated a significant upregulation of VEGF expression during the transition from normal oral epithelium through dysplasia to invasive OSCC, but no correlation was found between VEGF expression and the grade of dysplasia, while Margaritescu et al[22], found a correlation between VEGF and the different degrees of dysplasia, to invasive carcinoma.

In the present work, GIII showed a slight improvement in the animal's general health. The pouch length (2.5-3.5cm) was increased compared to GII due to reduction of the inflammatory infiltration and distal necrosis. A relatively slight decrease in size of the papillomatous lesions was observed. These findings conflicted on H&E staining in which five hamsters revealed different degrees of epithelial dysplasia {(moderate (10%), severe (20%) or CIS (20%)}XZ+5987\]*/-* while the-e other five hamsters showed superficial invasion of well

differentiated SCC (50%), not extended to deeper areas (DOI=1.8mm).

In the current study, IHC staining of GIII showed positive cytoplasmic expression of VEGF (51.80 %) that was seen throughout the epithelial layers and invading tumor cells, that showed highly significantly expression compared to GII (p value < 0.001).

These results may be attributed to that; nivolumab is immune check point inhibitor capable of specific inhibition of PD-1 signal that was sufficient to reduce the invasive lesions. This is in line with results of other investigators[23, 24].

Lee and Sunwoo[25] explained that, blocking the tumor-infiltrating lymphocytes (TILs) with anti-PD-L1 and anti-PD-1 antibodies partially restored interferon (IFN)-g secretion by the TILs incubated with the cancer cells, These results indicated that, PD-L1 expression on cancer cells may function as a mechanism by which they evade immunosurveillance and provide a cause for targeting the PD-1 axis. Furthermore, VEGF modulates anti-tumor immune responses through poor antigen presentation due to inhibition of dendritic cell maturation, interfering with T-cell trafficking and creating an immune suppressed tumor microenvironment through myeloid-derived suppressor cells and T-rig stimulation[26]. Amin et al[8] found that, VEGF in the tumor micro-environment was shown to increase expression of inhibitory checkpoints, PD-1, CTLA-4, TIM3, and LAG3, which was shown to be reversed by antibodies against VEGFR-2.

In the current study, GIV showed almost the same results as GIII. These results are in agreement with Paik et al[9] whom reported that, the tumor weight of the axitinib-treated group had significantly decreased by 50% compared with controls. Daily monitoring of animals throughout the therapy showed acceptable tolerability with no unfavorable side effects such as changes in body weight, mobility, posture, or feeding habits. In the present study, IHC staining of GIV showed positive cytoplasmic expression of VEGF (42.40 %) that was seen throughout the epithelial layers and invading tumor cells, which showed highly significantly expression compared to GII (p value < 0.001). These results agree with that of other investigators [9, 27].

Paul L. et al[28] stated that axitinib varies significantly when compared to other anti-angiogenic drugs in that it targets multiple isoforms of VEGFR (VEGFR1, VEGFR2, and VEGFR3) as well as c-Kit. The greater targeting of VEGFR especially leads to the possibility of having greater anti-angiogenic activity and hence clinical efficacy. Furthermore, in a phase 2 study of patients with heavily pretreated unresectable HNSCC, axitinib demonstrated an improvement in 6-month overall survival in comparison with historical controls (70% vs 50%). In addition, treatment resulted in significant response rates and lower rates of severe toxicities[29].

In the present study, GV as a combination group showed marked improvement in animal's general health compared to nivolumab G or axitinib G alone. There was a significant increase of the pouch's length (3.5 - 4.5cm) due to marked decrease of distal necrosis and inflammatory infiltration. Also, there was marked decrease in the size of exophytic masses in GV when compared to the animals treated with nivolumab or axitinib only. These findings conflicted on H&E staining which revealed different degrees of epithelial dysplasia {mild (10%), moderate (30%), severe (20%) or CIS (10%)} in addition to well differentiated SCC (30%) which was juxta-epithelial and not extended to the deeper C.T (DOI=0.8mm) with increased amount of keratin formation. The CT showed marked increase thickness of striated muscle layer and the tumor masses were mostly replaced by proliferated fibrous tissue with more collagen deposition.

These findings reflected the beneficial effect of combining nivolumab with axitinib in order to achieve these positive results. Several researchers have suggested that anti-angiogenic drugs can normalize tortuous and disorganized tumor vessels, thereby

theoretically enhancing the function of anti-PD-1 antibodies. Presently, the combination of anti-angiogenic drugs and anti-PD-1 antibodies has been tested in clinical trials for many solid tumors, and promising results have been obtained. The combination of nivolumab and anti-angiogenic drugs has been evaluated in patients with recurrent ovarian cancer. In small-scale phase 2 trial, the objective response rate to nivolumab and anti-angiogenic drugs was 28.9% in the entire cohort (40.0% in platinum-sensitive patients and 16.7% in platinum-resistant individuals), indicating that a fraction of patients might achieve a long-term benefit from the combination[30]. Motzer et al[31]found that, patients who received a combination of immune checkpoint inhibitor plus axitinib had longer progression-free survival and a higher objective response rate than those who received sunitinib.

In the present study, IHC staining of GV showed positive cytoplasmic expression of VEGF (26.80 %) that was seen throughout the epithelial layers and invading tumor cells, which showed highly significant difference compared to GII as well as to either GIII or GIV (p value < 0.001). This is in line with that shown by positive phase III studies have led to recent approvals by the FDA for dual PD-1/PD-L1 and anti-VEGF combinations in renal cell carcinoma (pembrolizumab plus axitinib, and avelumab plus axitinib), endometrial carcinoma (pembrolizumab plus lenvatinib), non-squamous NSCLC (atezolizumab, bevacizumab and chemotherapy), and HCC, suggesting a potential broad clinical utility of this combination strategy[32, 33].

Five Phase III studies have been initiated to evaluate various combinations of VEGF or VEGFR inhibitors plus either PD-1 or PD-L1 antibodies in patients with advanced RCC, of which three have been published[31,34]. Based on the results of JAVELIN 101 and KEYNOTE-426, combination treatment with either pembrolizumab or avelumab plus axitinib is now considered a standard of care in frontline advanced RCC[35]. Hack et al[36] concluded that, Combined blockade of PD-L1 and VEGF pathways represents a significant therapeutic advance in cancer treatment. The immunomodulatory role of VEGF, now well described by data from preclinical and translational studies as well as randomized clinical trials, provides a compelling reason to continue the study of anti-VEGF and immune checkpoint therapies across the cancer spectrum.

Ramjiawan et al[37] found that, judicious dosing of anti-angiogenic treatment can transiently normalize the tumor vasculature by decreasing vascular permeability and improving tumor perfusion and blood flow, and synergize with immunotherapy in this time-window. However, anti-angiogenics may excessively prune tumor vessels in a dose and time-dependent manner, which induces hypoxia and immunosuppression, including increased expression of the immune checkpoint programmed death receptor ligand (PD-L1). Sheng et al[38]reported the preliminary safety and efficacy results of the combination of PD-1 blockade with a VEGFR small-molecule inhibitor in patients with chemotherapy-treated mucosal melanoma, which demonstrate a manageable safety profile and durable antitumor activity.

CONCLUSION

Combination of axitinib-nivolumab significantly inhibits tumor progression in DMBA induced HBP carcinoma. Axitinib makes an important and useful contribution with emerging with novel targeted immunomodulatory agents such as with nivolumab. The approval of immunotherapy as an effective modality in the treatment of OSSC has state a new era in combinatorial therapeutic approaches for this disease. While the use of combination therapy forms an intriguing forefront for the treatment of OSCC, we have yet to understand how immunotherapy and anti-angiogenic therapy interact with each other to create an anti-tumor effect. Further investigations need to appreciate both the benefits and the risks posed by inhibiting these alternative therapeutic pathways and how they impact the tumor microenvironment.

REFERENCES

1. Sun Y, Ren J, Wang FJJoB, Toxicology M. [6]-Gingerol impedes 7, 12-dimethylbenz (a) anthracene-induced inflammation and cell proliferation-associated hamster buccal pouch carcinogenesis through modulating Nrf2 signaling events. 2021;35(4):e22689.
2. Al-Dosoki MA A-AA, Omar AMZ, Zouair MGA. Flow cytometric assessment of nivolumab and/or epigallocatechin-3-gallate on cancer stem cells of DMBA induced hamster buccal pouch carcinoma. Medical Science. 2021;25(118):3206-21.
3. Carosella ED, Ploussard G, LeMaoult J, Desgrandchamps FJEu. A systematic review of immunotherapy in urologic cancer: evolving roles for targeting of CTLA-4, PD-1/PD-L1, and HLA-G. 2015;68(2):267-79.
4. Bai R-L, Chen N-F, Li L-Y, Cui J-WJCMJ. A brand new era of cancer immunotherapy: breakthroughs and challenges. 2021;134(11):1267-75.
5. Saung MT, Pelosof L, Casak S, Donoghue M, Lemery S, Yuan M, et al. FDA approval summary: nivolumab plus ipilimumab for the treatment of patients with hepatocellular carcinoma previously treated with sorafenib. 2021;26(9):797-806.
6. Schlüter A, Weller P, Kanaan O, Nel I, Heusgen L, Höing B, et al. CD31 and VEGF are prognostic biomarkers in early-stage, but not in late-stage, laryngeal squamous cell carcinoma. 2018;18(1):1-8.
7. Akbarian M, Bertassoni LE, Tayebi LJC, Sciences ML. Biological aspects in controlling angiogenesis: current progress. 2022;79(7):349.
8. Amin A, Hammers HJFii. The evolving landscape of immunotherapy-based combinations for frontline treatment of advanced renal cell carcinoma. 2019;9:3120.
9. Paik ES, Kim T-H, Cho YJ, Ryu J, Choi J-J, Lee Y-Y, et al. Preclinical assessment of the VEGFR inhibitor axitinib as a therapeutic agent for epithelial ovarian cancer. 2020;10(1):4904.
10. Lu L, Saha D, Martuza RL, Rabkin SD, Wakimoto HJ-Jon-o. Single agent efficacy of the VEGFR kinase inhibitor axitinib in preclinical models of glioblastoma. 2015;121(1):91-100.
11. Hu-Lowe DD, Zou HY, Grazzini ML, Hallin ME, Wickman GR, Amundson K, et al. Nonclinical antiangiogenesis and antitumor activities of axitinib (AG-013736), an oral, potent, and selective inhibitor of vascular endothelial growth factor receptor tyrosine kinases 1, 2, 3. 2008;14(22):7272-83.
12. Faisal M, Abu Bakar M, Sarwar A, Adeel M, Batool F, Malik KI, et al. Depth of invasion (DOI) as a predictor of cervical nodal metastasis and local recurrence in early stage squamous cell carcinoma of oral tongue (ESSCOT). PloS one. 2018;13(8):e0202632.
13. Kim S-W, Roh J, Park C-SJJop, medicine t. Immunohistochemistry for pathologists: protocols, pitfalls, and tips. 2016;50(6):411-8.
14. El-Hossary WH, Hegazy E, El-Mansy MN. Topical Chemopreventive Effect of Thymoquinone Versus Thymoquinone Loaded on Gold Nanoparticles on Dmba-Induced Hamster Buccal Pouch Carcinogenesis (Immunohistochemical Study). Egyptian Dental Journal. 2018;64(4-October (Oral Medicine, X-Ray, Oral Biology & Oral Pathology)):3523-33.
15. Sophia J, Kowshik J, Mishra R, Nagini S. Nimbolide, a neem limonoid inhibits phosphatidyl inositol-3 kinase to activate glycogen synthase kinase-3β in a hamster model of oral oncogenesis. Scientific reports. 2016;6(1):1-13.
16. Hassan MM, El-Hossary WH, Hanafi R. Anti-inflammatory Thymoquinone and Muscle Regeneration in the Hamster Buccal Pouch-Induced Dysplasia. 2020.
17. Rundhaug JE, Fischer SM. Molecular mechanisms of mouse skin tumor promotion. Cancers. 2010;2(2):436-82.
18. Manoharan S, Sindhu G, Nirmal MR, Vetrichelvi V, Balakrishnan S. Protective effect of berberine on expression pattern of apoptotic, cell proliferative, inflammatory and angiogenic markers during 7, 12-dimethylbenz (a) anthracene induced hamster buccal pouch carcinogenesis. Pakistan Journal of Biological Sciences: PJBS. 2011;14(20):918-32.
19. Gouda AM, El-Didi FH, Darwish ZE, Zeitoun IM. EXPRESSION OF VASCULAR ENDOTHELIAL GROWTH FACTOR IN ORAL SQUAMOUS CELL CARCINOMA: A CLINICOPATHOLOGICAL STUDY. Alexandria Dental Journal. 2017;42(2):187-92.
20. Martano M, Restucci B, Ceccarelli DM, Lo Muzio L, Maiolino P. Immunohistochemical expression of vascular endothelial growth factor in canine oral squamous cell carcinomas. Oncology letters. 2016;11(1):399-404.
21. Johnstone S, Logan R. Expression of vascular endothelial growth factor (VEGF) in normal oral mucosa, oral dysplasia and oral squamous cell carcinoma. International journal of oral and maxillofacial surgery. 2007;36(3):263-6.
22. Mărgăritescu C, Pirici D, Stîngă A, Simionescu C, Raica M, Mogoantă L, et al. VEGF expression and angiogenesis

in oral squamous cell carcinoma: an immunohistochemical and morphometric study. Clinical and experimental medicine. 2010;10(4):209-14.

23. Chen Y, Li Q, Li X, Ma D, Fang J, Luo L, et al. Blockade of PD-1 effectively inhibits in vivo malignant transformation of oral mucosa. 2018;7(2):e1388484.
24. Tada H, Takahashi H, Kawabata-Iwakawa R, Nagata Y, Uchida M, Shino M, et al. Molecular phenotypes of circulating tumor cells and efficacy of nivolumab treatment in patients with head and neck squamous cell carcinoma. 2020;10(1):21573.
25. Lee Y, Sunwoo JJJfIoC. PD-L1 is preferentially expressed on CD44+ tumor-initiating cells in head and neck squamous cell carcinoma. 2014;2(3):1-.
26. Yang J, Yan J, Liu B. Targeting VEGF/VEGFR to modulate antitumor immunity. Frontiers in Immunology. 2018;9:978.
27. Zheng X, Fang Z, Liu X, Deng S, Zhou P, Wang X, et al. Increased vessel perfusion predicts the efficacy of immune checkpoint blockade. The Journal of clinical investigation. 2018;128(5):2104-15.
28. Swiecicki PL, Zhao L, Belile E, Sacco AG, Chepeha DB, Dobrosotskaya I, et al. A phase II study evaluating axitinib in patients with unresectable, recurrent or metastatic head and neck cancer. 2015;33:1248-56.
29. Swiecicki PL, Bellile EL, Brummel CV, Brenner JC, Worden FPJC. Efficacy of axitinib in metastatic head and neck cancer with novel radiographic response criteria. 2021;127(2):219-28.
30. Liu JF, Herold C, Gray KP, Penson RT, Horowitz N, Konstantinopoulos PA, et al. Assessment of combined nivolumab and bevacizumab in relapsed ovarian cancer: a phase 2 clinical trial. 2019;5(12):1731-8.
31. Motzer RJ, Penkov K, Haanen J, Rini B, Albiges L, Campbell MT, et al. Avelumab plus axitinib versus sunitinib for advanced renal-cell carcinoma. New England Journal of Medicine. 2019;380(12):1103-15.
32. Finn RS, Qin S, Ikeda M, Galle PR, Ducreux M, Kim T-Y, et al. Atezolizumab plus bevacizumab in unresectable hepatocellular carcinoma. New England Journal of Medicine. 2020;382(20):1894-905.
33. Makker V, Rasco D, Vogelzang NJ, Brose MS, Cohn AL, Mier J, et al. Lenvatinib plus pembrolizumab in patients with advanced endometrial cancer: an interim analysis of a multicentre, open-label, single-arm, phase 2 trial. The Lancet Oncology. 2019;20(5):711-8.
34. Rini BI, Powles T, Atkins MB, Escudier B, McDermott DF, Suarez C, et al. Atezolizumab plus bevacizumab versus sunitinib in patients with previously untreated metastatic renal cell carcinoma (IMmotion151): a multicentre, open-label, phase 3, randomised controlled trial. The Lancet. 2019;393(10189):2404-15.
35. Huang JJ, Hsieh JJ, editors. The therapeutic landscape of renal cell carcinoma: from the dark age to the golden age. Seminars in nephrology; 2020: Elsevier.
36. Hack SP, Zhu AX, Wang Y. Augmenting anticancer immunity through combined targeting of angiogenic and PD-1/PD-L1 pathways: challenges and opportunities. Frontiers in Immunology. 2020;11:598877.
37. Ramjiawan RR, Griffioen AW, Duda DG. Anti-angiogenesis for cancer revisited: Is there a role for combinations with immunotherapy? Angiogenesis. 2017;20(2):185-204.
38. Sheng X, Yan X, Chi Z, Si L, Cui C, Tang B, et al. Axitinib in combination with toripalimab, a humanized immunoglobulin G4 monoclonal antibody against programmed cell death-1, in patients with metastatic mucosal melanoma: an open-label phase IB trial. Journal of Clinical Oncology. 2019;37(32):2987.